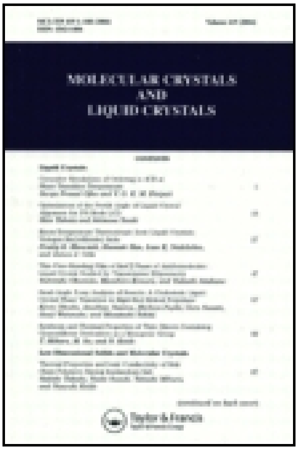

Molecular Crystals and Liquid Crystals
Publication details, including instructions for authors and subscription information:
http://www.tandfonline.com/loi/gmcl20

Catalytic Polymerization Of Ethylene, 1,4-Butadiene, and Ethylene Oxide with No Solvent: Heat Effects, Kinetics, and Mechanisms

Victor E. Ostrovskii [a] & V. A. Khodzhemirov [a]
[a] Karpov Institute of Physical Chemistry, ul. Vorontsovo Pole 10, Moscow, 103064, Russia

To cite this article: Victor E. Ostrovskii & V. A. Khodzhemirov (2002): Catalytic Polymerization Of Ethylene, 1,4-Butadiene, and Ethylene Oxide with No Solvent: Heat Effects, Kinetics, and Mechanisms, Molecular Crystals and Liquid Crystals, 390:1, 67-78

To link to this article: http://dx.doi.org/10.1080/10587250216154

Mol. Cryst. Liq. Cryst., Vol. 390, pp. 67–78
Copyright © 2003 Taylor & Francis
1542-1406/03 $12.00 + .00
DOI: 10.1080/15421400390193422

CATALYTIC POLYMERIZATION OF ETHYLENE, 1,4-BUTADIENE, AND ETHYLENE OXIDE WITH NO SOLVENT: HEAT EFFECTS, KINETICS, AND MECHANISMS

Victor E. Ostrovskii, and V. A. Khodzhemirov*
Karpov Institute of Physical Chemistry, ul. Vorontsovo Pole 10,
Moscow, 103064, Russia

The processes of solid polyethyleneoxide (PEO), polyethylene (PE), and trans–1,4-polybutadiene (PB) formation at solid catalysts in gas-solid systems with no solvent are studied. For a monomer pressure of 760 Torr, maximum rates of $1.5 \cdot 10^{-7}$, $1.2 \cdot 10^{-5}$, *and* $4 \cdot 10^{-7}$ *(mol/s* cm^3*) are fixed for* C_2H_4O, C_2H_4, *and 1,4-*C_4H_6 *polymerization, respectively; therewith, potentialities of intensification of the reactions are not exhausted. The* ΔH^0_{298} *values measured for the reaction* $(MON)_{(gas)} = (1/n)(\text{-}MON\text{-})_{n(solid)}$ *(MON is a monomer molecule) are* -107.5 ± 2.5, -112.5 ± 2.5, *and* -140.5 ± 3.8 *(kJ/mol) for PE, PB, and PEO, respectively.*

Keywords: polymerization at dry catalysts; polymerization enthalpy; polyethyleneoxide polyethylene; 1,4-polybutadiene

INTRODUCTION

Catalytic production of polymers in gas-solid systems would open very alluring prospects for simplification of the technology and quality control and also for the pollution abatement; it is also essential to coating films on to solids. Such a mode of polymerization allows measurements of the heat effects for gaseous monomer → solid polymer reactions with no side heat effects.

---

*Corresponding author. E-mail: vostrov@cc.nifhi.ac.ru

EXPERIMENTAL

Materials

Source liquid ethylene oxide (EO) produced through catalytic oxidation of C_2H_4 contained 99.5% of EO. It was freed of dissolved gases by repeated cycles of freezing to 77 K, pumping, isolation from the pump, and heating to 298 K and was dried through short-term exposure to solid KOH at 195 K.

Source ethylene (E) produced from C_2H_5OH was purged through pyrolusite and molecular sieves and freed, as EO, of dissolved gases.

Chromatography-pure 1,4-butadiene (B) was dried over $Si(C_2H_5)_4$ and degassed.

Fused KOH (8.3 g) specified as "chemically pure" was used as the catalyst of EO polymerization. The KOH lens were broken to grains 1–2 mm in size, poured into the calorimetric ampoule, and dried at 298 K through several-hour exposure to a trap cooled to 77 K at about $2 \cdot 10^{-6}$ Torr.

The catalyst for E and B polymerization was prepared on the basis of α-$TiCl_3$ obtained from $TiCl_4$ through its reduction by metal Ti. In an air-free medium, powdered α-$TiCl_3$ was processed with vapors of $Al(CH_3)_3$ at 298 K and 10 Torr up to termination of the gas- and heat-evolution and then was pumped off to about 0.001 Torr.

The surfaces of α-$TiCl_3$ processed with a metal-alkylate and of dry KOH were measured with no contact with the atmosphere. The technique of Kr adsorption at 77 K and the computation according to BET, with $\sigma_0 = 19.5\,\text{Å}^2$ and $p_0 = 3.175$ Torr were used. The specific surface areas were found to be equal to 5.75 and 0.13 m^2/g for α-$TiCl_3$ processed with $Al(CH_3)_3$ and for KOH, respectively.

Installation

The set of installation includes a glass vacuum apparatus supplied with a mercury diffusion pump and a "FOSKA" microcalorimeter intended for heat measurements at constant temperatures.

Vacuum Apparatus

The principal block of the glass vacuum apparatus is given in Figure 1.

Two calorimetric ampoules, the test (1) and comparative (2) ones equal to each other in their size and mass, contain a weight of KOH and a weight of glass spheres of the same heat capacity, respectively. The glass ampoules are housed into the calorimetric cells of the calorimeter (3). For thinning the catalyst layer and making all its elements to be equiaccessible for gaseous molecules, the solid sample is put in a space 2.5 mm in width between the glass porous filter and the wall of the ampoule (Fig. 1b). The

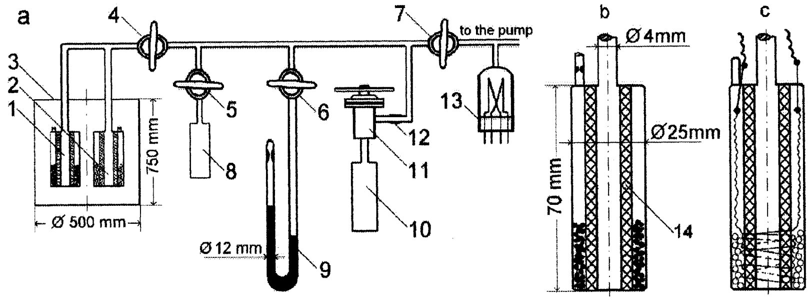

FIGURE 1 (a) Glass apparatus, (b) test calorimetric ampoule, (c) calibrating calorimetric ampoule: (1) test ampoule; (2) comparative ampoule; (3) calorimeter; (4)–(7) glass taps; (8) tube for freezing of monomers; (9) Hg manometer; (10) steel tube for monomers; (11) steel tap; (12) kovar bridge; (13) manometer; (14) glass porous filter.

catalyst (and the glass spheres) is poured into the ampoule through the small tube terminal then sealed. All the apparatus volumes bounded with the taps are calibrated. The calibration error does not exceed 1.5%.

Microcalorimeter

The first model of the microcalorimeter was described earlier [1], and the last model modified is shown in Figure 2.

This is a twin differential nonisothermal-nonadiabatic “FOSKA” microcalorimeter. Our instruments fall into the so-called isoperibol calorimeters. The design of the thermostating system is analogous to that described earlier by Calvet and Prat [2]. Instead of thermocouple batteries used in the calorimeters described in [2], our instruments contain Pt thermometers as sensors of the heat fluxes. This fact leads to some peculiarities in the procedure of measuring of the heat fluxes [3].

The FOSKA microcalorimeters allow realization of the zero line with fluctuations within $0.02 \cdot 10^{-6}$ V ($4 \cdot 10^{-6}$ W) and measurements of the heat effects with an accuracy of 1–1.5% at a recorder scale of about $1 \cdot 10^{-2}$ J/cm^2. Calibration of the calorimeter is performed with the Joule effect by using calibrating calorimetric ampoule (Fig. 1c) analogous to the test and comparative calorimetric ampoules but containing additionally a constantan heater.

Modes of Operating

Polymerization is performed at 298 K in the ampoule (1) housed in thecalorimeter. During the experiments, monomers are consumed from the closed volume bounded with the taps (7) and (11). The monomer amount

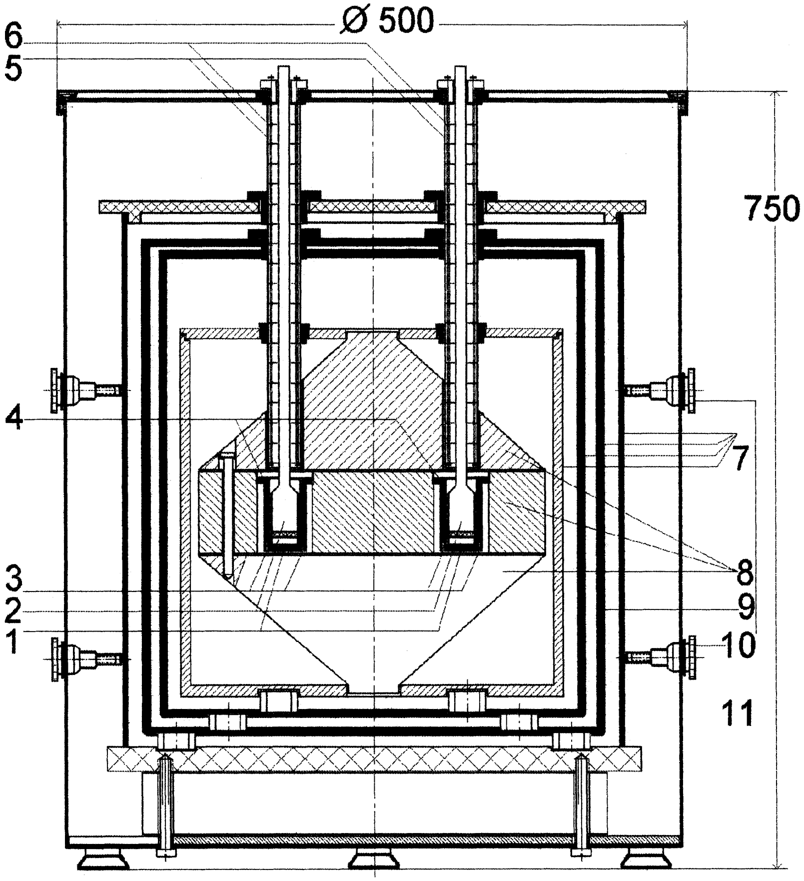

FIGURE 2 Design of the calorimeter: 1-calorimetric vessel, 2-calorimetric ampoule, 3-finger Pt-wire resistance thermometers capsulated in light-wall ceramic sealed tubes, 4-glass (or porcelain) rings, 5-glass (or porcelain) tubes, 6-whatnot devices, 7-canisters, 8-metal block, 9-heater of the thermostating system, 10-detent, 11-lightweight insulating material.

consumed is controlled with the manometer (9) by using a horizontal microscope graduated in 0.02 mm. During each experiment, the accuracy of the pressure reduction measurement does not exceed 0.2%. Each experiment proceeds for 1–6 h. In the course of each experiment, the monomer pressure changes around its mean value by no more than 5–7.5%; therefore, it is possible to take approximately that the measurements are performed constant pressures.

Before the experiments, we evacuate the volume over the catalyst, take a portion of dry monomer from the tube (8) into the evacuated volume between the taps (4)-(5)-(6)-(7)-(11), measure the pressure by the manometer (9), compute the monomer vapor amount, and turn on the tap (4). Polymerization starts, and the recorder of the calorimetric device begins to write a thermokinetic curve away from the zero line.

To interrupt the polymerization process, we cool the tube (8) down to 77 K, freeze the residual monomer, and turn off the tap (4). After that, we heat the tube (8) to the room temperature, measure the residual pressure in the volume between the taps (4)-(7)-(11), and compute the amount of the monomer transformed to the polymer. In the meantime, the thermokinetic curve returns to the zero line.

Thereupon, we turn on the tap (4) and perform a new experiment or, before that, we dry an additional amount of the monomer and, cooling the tube (8) down to 77 K, add this additional monomer to the monomer amount remained in the tube (8) after the previous experiment.

The surface area under the thermokinetic curve characterizes the heat of polymerization. During the period of near-stationary polymerization, excluding transient time intervals after turning on and off the tap (4), the thermokinetic curve reflects the rate of polymerization. Indeed, at any instant, its deviation from the zero line is proportional to the heat flux that is proportional to the reaction rate. Basing on this property of the calorimetric device, we compute the rate of polymerization for the time moment corresponding to the middle of each experiment.

Molecular Weight

The number-average molecular weight (M) is computed by equations: for polyethyleneoxide (PEO), $[\eta]$ (water, $308\,\mathrm{K}) = 6.4\cdot 10^{-5}\cdot \mathrm{M}^{0.82}$, and polyethylene (PE), $[\eta]$ (decahydronaphthalene, $408\,\mathrm{K}) = 4.6\cdot 10^{-4}\cdot \mathrm{M}^{0.73}$, where $[\eta]$ is the characteristic viscosity.

The maximum M values for PE produced at the (α-$\mathrm{TiCl_3} + \mathrm{Al(CH_3)_3}$) samples and for PEO produced at the KOH samples are equal to about $1\cdot 10^6$ and $1.26\cdot 10^4$, respectively. The M of the polymers thus produced appears to be regulated. For trans-1,4-polybutadiene (PB), the M value is not measured since the polymer is not soluble.

RESULTS

Kinetics of E and B Polymerization

The maximum rate observed for E and B polymerization at 298 K and 760 Torr is equal to $1.2\cdot 10^{-5}$ and $4\cdot 10^{-7}$ mol/s cm^3, respectively.

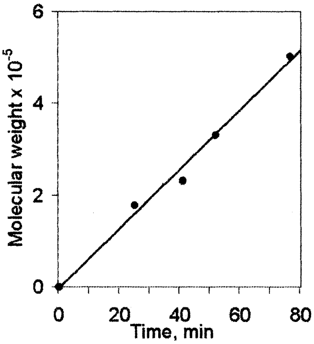

FIGURE 3 The M of PE against the duration of polymerization.

The tenfold variations in the monomer pressure and catalyst weight show that the rate is proportional to these parameters. Polymerization of E proceeds up to the total consumption of the monomer.

If, on a day X, the rate (r_X) of polymerization is measured at a pressure P_X and, after that, the process is interrupted by full freezing of the monomer vapor from the volume over the catalyst, on the day (X+1) at the same pressure P_X, $r_{(X+1)} \approx r_X$. At any sample of the catalyst, polymerization of E and B can be provided in the alternate mode. Thus, it seems reasonable to say that the polymerization proceeds through the mechanism of "living" polymers.

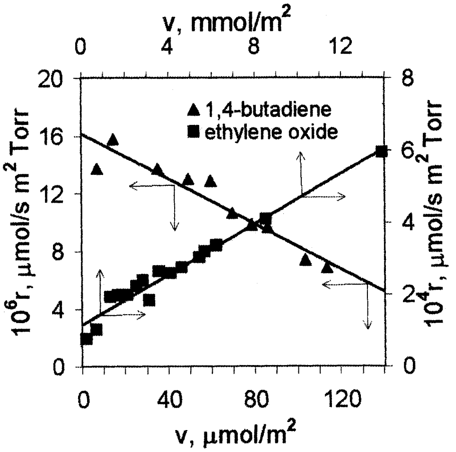

FIGURE 4 The rates of EO and B polymerization against the degree of polymerization.

For several hours, the rate of E polymerization normalized to the pressure is nearly constant and then it decreases progressively.

The number-average molecular weight of PE increases progressively with time up to about 10^6. Figure 3 shows that, for the first 1.5 h, the M value is closely proportional to the duration of the process. Then, the rate of increasing of M and the rate of polymerization begin to decrease. The rate of B polymerization decreases as the polymer amount at the catalyst surface increases (Fig. 4). At a degree of polymerization of about 100 μmol/m^2, the rate of the process is less than the initial one by a factor of two.

Kinetics of EO Polymerization

Two series of the experiments with the initial pressures decreasing in a stepwise manner from one experiment to another in each of the series and two out-of-series experiments were performed. In the experiments, the mean vapor pressure varies from 127 to 368 Torr. The equilibrium is shifted to formation of the polymer; the process of polymerization decreases the pressure of the monomer to zero.

The polymerization rate is proportional to the monomer pressure [4].

The maximum rate of EO polymerization observed at 298 K and extrapolated to 760 Torr is equal to $1.5 \cdot 10^{-7}$ mol/s cm^3.

It is found that the rate of EO polymerization increases with the degree of polymerization. Such a conclusion follows from Figure 5. In this Figure, the polymerization rates measured in the experiments performed at 352 ±15 Torr and at different degrees of polymerization are given. The rate

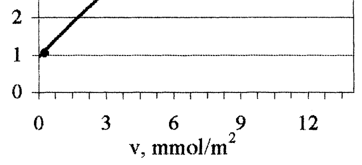

FIGURE 5 Illustration of the effect of increasing of the rate of EO polymerization with the degree of polymerization.

values are normalized to the rate measured at the KOH surface free of the polymer. We denote the rates normalized by α and term α the coefficient of increasing of polymerization rate.

At a degree of polymerization of about 14 mmol/m^2 (80 mg of PEO per 1 g of KOH), we have $\alpha = 7.7$.

For any experiment, the rate of EO polymerization

$$r = k\alpha P, \tag{1}$$

where P is the monomer pressure and α taken from Figure 5 relates to the degree of polymerization in the middle of the experiment under consideration. The validity of Eq. (1) is seen from Figure 4. Figures 4 and 5 give $k = 0.863 \pm 0.90$ µmol/s Torr.

Heats of Polymerization

Table 1 contains the molar heat effects of polymerization.

From Table 1 it follows that the ΔH^0_{298} values for reactions $(MON)_{(gas)} = 1/n(\text{-MON-})_{n(solid)}$, where MON is a monomer molecule E, B, or EO, are equal to −107.5 ± 2.5, −112.5 ± 2.5, and −140.5 ± 3.8 (kJ/mol), respectively.

TABLE 1 Heats of Polymerization, 298 K

N	Monomer volume, cm^3, ntp	Molar heat, kJ/mol	N	Monomer volume, cm^3, ntp	Molar heat, kJ/mol
C_2H_4O			16	17.43	138.9
1	9.53	136.4	C_2H_4		
2	13.47	141.5	1	29.30	106.0
3	9.00	128.5	2	31.40	105.5
4	9.29	143.5	3	29.92	111.5
5	11.48	135.9	4	12.18	108.0
6	7.24	137.4	5	30.50	107.5
7	7.99	136.5	1,4-C_4H_6		
8	7.58	135.0	1	9.195	114.5
9	13.54	139.6	2	9.935	110.0
10	12.35	147.5	3	9.350	115.3
11	12.53	147.9	4	7.965	110.0
12	12.33	140.7	5	6.045	108.7
13	13.27	140.6	6	5.530	113.2
14	12.56	139.5	7	5.500	112.5
15	21.04	141.3	8	5.740	114.6

DISCUSSION

Rates and Mechanisms of the Processes

According to the 4th law by P. Weisz, catalytic researches and technologies are advanced if the rates of the processes are no less than 10^{-5}–10^{-6} mol/s·cm^3. The possibility of realization of catalytic polymerization in the gas-solid system is open to question. We observed the rate of E polymerization equal to $1.2 \cdot 10^{-5}$ mol/s·cm^3, but the mode of realization of this rate is rather irregular. The maximum observed rates of B and EO polymerization are as low as $4 \cdot 10^{-7}$ and $1.5 \cdot 10^{-7}$ mol/s·cm^3, respectively. However, two peculiarities favor setting the ultimate decision aside for the time being. First, the potentialities of intensification of these processes are not exhausted and the results obtained allow identification of some parameters accessible to be optimized, namely, the temperature and the specific surface area of the catalyst. Second, in future, some advantages of the technology with no solvent and some peculiarities of the polymers thus produced may appears to be the governing factor.

The results obtained give grounds for discussing some questions of the mechanisms of polymerization in the gas-solid systems. At first, we will discuss the results relating to EO polymerization and then will apply the same approaches to the data on E polymerization.

As was said in the preceding section, with the 8.3-g catalyst weight characterized by a specific surface area of 0.13 m^2/g, we observed at 298 K a polymerization rate of $5.95 \cdot 10^{-4}$ μmol/s m^2 Torr at a degree of polymerization of 79.5 mg PEO/g KOH. PEO obtained had the number-average molecular weight $M = 12\,600$. These data allowed us to estimate the number δ of active surface centers of KOH ($3.80 \cdot 10^{18}$ g^{-1} that is $2.92 \cdot 10^{19}$ m^{-2}) and the number ω of reaction acts occurring at 298 K on one active center of the catalyst surface (0.0093 s^{-1} at 760 Torr). For these computations, we took that δ is equal to the number of the average polymer chains, i.e., that each active center produces a polymer chain.

In other words, at each active center, one polymerization act proceeds, on the average, every 107 s. For comparison, we note that, according to the molecular-kinetic theory, the number of collisions of gas molecules with a surface of 1 cm^2 at 298 K and 760 Torr for 107 s is about $2.45 \cdot 10^{29}$. If a crystal face contains $1.4 \cdot 10^{19}$ surface centers per 1 cm^2, the number of collisions of gas molecules with a surface center under such conditions is equal to $1.75 \cdot 10^{10}$.

It is clear that the $\delta \cdot \omega$ product characterizes the catalytic activity. For EO polymerization at a pressure of 760 Torr, we obtained the number of the polymerization acts $\delta \cdot \omega = 2.72 \cdot 10^{17}$ s^{-1}m^{-2}. In [5], this product is given for liquid-phase EO polymerization with different earth-metal hydroxides as catalysts. Hydroxides of beryllium and magnesium are most active; at 298 K, the $\delta \cdot \omega$ values computed for 1 m^2 of their surface areas are equal to $0.26 \cdot 10^{17}$ and $1.0 \cdot 10^{16}$, respectively. It is seen that the specific catalytic activity of KOH in gas-phase polymerization is significantly higher than that of $Be(OH)_2$ and $Mg(OH)_2$ in liquid-phase polymerization.

The fact that the δ values obtained for liquid-phase polymerization in [5] and for gas-phase polymerization in our work are around the standard numbers of atoms located at 1 m^2 of crystal faces is noteworthy. In [5], for polymerization at different hydroxides, these values are between 10^{17} and 10^{18}. In our case, the corresponding value is twice as large as the value $1.4 \cdot 10^{19}$ characterizing the maximum number of atoms located at 1 m^2 of crystal latitudes.

The results on E polymerization lead to a mean number of polymer chains at about $2 \cdot 10^{16}\,m^{-2}$. This value is three orders of magnitude less than the number of atoms at crystal faces with surface areas of 1 m^2. Under conditions of the maximum observed rate of E polymerization, at 760 Torr and 298 K, each active center "worked", on the average, every 0.040 s, i.e., for each second, each polymer chain increased by 25 molecules.

One more phenomenon giving grounds for the hypothesis that block-copolymers can be obtained in the solid-gas systems should be mentioned. Following ethylene polymerization and evacuation of the nonpolymerized residual monomer, the butadiene admission into the empty volume over the catalyst leads to formation of 1,4-polybutadiene, and, conversely, following butadiene polymerization and evacuation of the residual monomer, the ethylene admission into this volume leads to formation of polyethylene. If polymerization proceeds in the orderly sequence: ethylene (1) – butadiene - ethylene (2), the initial rate of ethylene (2) polymerization is significantly slower than the terminal rate of ethylene (1) polymerization. Apparently, these results show that the masses of the blocks can be regulated through variation of the duration of polymerization.

A possible explanation of the dependences of the polymerization rate (PR) on the degree of polymerization observed for the systems studied is as follows.

Consider the initial step of polymerization at unit pressure of the monomers and unit surface of catalysts. We use the ratio (ν_{orig}/ν_{add}), where ν_{orig} and ν_{add} are the frequencies of acts of consumption of the gas molecules for polymer chain generation at the surface and for polymerization, respectively. In the α-$TiCl_3$-$Al(CH_3)_3$-E-PE system, the (ν_{orig}/ν_{add}) ratio is small, and the growing chains originated at the beginning of the process hamper access of monomer molecules to the surface and origination of new chains. The excessively high value of the specific surface area resulted in too small diameters of the clearances (pores) between the catalyst particles is the additional cause hampering approaching of the monomer molecules to the surface. Therefore, for E, after the beginning of the process, the PR is stabilized for several minutes and remains nearly constant for several hours, since all the chains grow with a nearly constant rate. Then, the chains begin to form balls or the quadratic recombination of the growing polymer chains becomes more frequent, and thus the PR diminishes.

In the α-$TiCl_3$-$Al(CH_3)_3$-B-PB system, the (ν_{orig}/ν_{add}) ratio is large, the chains generated quickly at the entire surface and grow all together. As a consequence of a high density of location of the polymer chains, the polymer packs quickly in the catalyst pores and this phenomenon stimulates the quadratic recombination of free-end valences of growing polymer chains and formation of bridge bonds between the adjacent polymer molecules. Therefore, the polymerization rate of butadiene decreases with time.

In the KOH-EO-PEO system, the (ν_{orig}/ν_{add}) ratio is of the order of one and, as some chains are growing, the others are originating. Thus, the number of the chains and, consequently, the PR increase in time. The KOH specific surface area is less than the specific surface of the α-$TiCl_3$-$Al(CH_3)_3$ system by a factor of about 45. Apparently, up to an M value of about 13000, the pore size in the KOH catalyst is reasonable for the monomer transport to the surface. Gradually, the number of surface centers free of polymer chains decreases and the surface becomes coated with the polymer. These phenomena initiate marked saturation of the plot in Figure 5.

According to our estimations, the numbers of the PEO and PE chains are about $3 \cdot 10^{19}$ and $2 \cdot 10^{16}$ (m^{-2}), respectively. The value $3 \cdot 10^{19}$ is of the same order as the number of lattice atoms at $1\,m^2$ of closely packed crystal faces, and the value $2 \cdot 10^{16}$ is three orders less than this number. This fact counts in favor of the above-given consideration.

Heats of Polymerization

Performance of polymerization in the gas-solid system presents a unique possibility for measuring the enthalpy change in the course of polymerization with no side heat effects, such as the heats of dissolution of the reactants during liquid-phase polymerization or the side heats caused by additives and impurities during combustion.

The enthalpy changes in the reactions $(MON)_{(gas)} = 1/n(\text{-MON-})_{n(solid)}$ (MON is a monomer molecule) at 298 K are equal to -107.5 ± 2.5 (I), -112.5 ± 2.5 (II), and -140.5 ± 3.8 (III) (kJ/mol) for PE, PB, and PEO, respectively. The I, II, and III values can be compared with the following data: -108.28, -93.60, and -119.9 (kJ/mol) (the last, for the reaction $(C_2H_4O)_{(gas)} = (1/n)\ (C_2H_4O)_{n(liquid)}$) obtained by using the heats of combustion [6,7] and [8] , respectively, and the tabulated heats of monomer vaporization.

The heat of EO vaporization at 298 K is equal to 24.94 kJ/mol [9]. Thus, for polymerization of liquid EO to solid PEO, $\Delta H_{298(\mathrm{liq.EO}\rightarrow\mathrm{sol.PEO})} = -115.76$ kJ/mol. From heats of combustion, $\Delta H_{(\mathrm{liq.EO}\rightarrow\mathrm{sol.PEO})} = -109.20$ kJ/mol was found [10]. It is seen that two last values are in rather good agreement to one another. At 372.1 K, for the process of liquid EO polymerization up to formation of PEO solved in EO, a value of -87.5 ± 2.1 kJ/mol was obtained [10]. A comparison of this value with our result is hampered by the fact that the value of the heat of PEO dissolution in EO is known only approximately. However, this value, in all likelihood, can not be reconciled rather closely with the value $\Delta H_{298(\mathrm{liq.EO}\rightarrow\mathrm{sol.PEO})} = -115.76$ kJ/mol given before.

REFERENCES

[1] Ostrovskii, V. E., Dobrovol'skii, N. N., Karpovich, I. R., & Frolov, F. Ya. (1968). *Zh. Fiz. Khim. (Rus. J. Phys. Chem.), 42*, 550.

[2] Calvet, E., Prat, H., & Skinner, H. (1963). *Recent Progress in Microcalorimetry*, Pergamon: New York.

[3] Ostrovskii, V. E. *J. Sci. Instr.* in print.

[4] Ostrovskii, V. E. & Khodzhemirov, V. A. *Plastics, Rubber, Composites-Processing and Applications*. in print.

[5] Krylov, O. V., Kushnerov, M. Ya., Markova, E. A., & Fokina, E. A. (1965). *Vysokomolekulyarnye Soedineniya, 7*, 984.

[6] Parks, G. S. & Mosker, H. P. (1963). *J. Polym. Sci., P. A., 1*, 1979.

[7] Nelson, R., Jessup, R., & Roberts, D. (1952). *J. Res. Nat. Bur. Stand., 48*, 275.

[8] Dainton, F. S. & Ivin, K. J. (1958). *Quart. Rev.*, London *12*, 61.

[9] Cox, J. D. & Pilcher, G. (1970). *Thermochemistry of Organic and Organometallic Compounds*, AP: London - New York.

[10] Kazanskii, K. S. & Entelis, S. G. (1965). *Izvestiya AN SSSR, Ser. Khim.*, 1089.